Chinese Chemical Letters 32 (2021) 3903–3906

Contents lists available at ScienceDirect

Chinese Chemical Letters

journal homepage: www.elsevier.com/locate/cclet

Communication

Self-assembly of amphiphilic peptides to construct activatable nanophotosensitizers for theranostic photodynamic therapy

Shuang Chen[a], Yongzhuo Liu[b], Ri Liang[a], Gaobo Hong[a], Jing An[a], Xiaojun Peng[a],
Wen-Heng Zheng[c,*], Fengling Song[a,d,*]

[a] *State Key Laboratory of Fine Chemicals, Dalian University of Technology, Dalian 116024, China*
[b] *Shandong Collaborative Innovation Center of Eco-Chemical Engineering, College of Chemical Engineering, Qingdao University of Science and Technology, Qingdao 266042, China*
[c] *Department of Medical Imaging, Cancer Hospital of China Medical University, Liaoning Cancer Hospital and Institute, Shenyang 110042, China*
[d] *Institute of Frontier and Interdisciplinary Science, Shandong University, Qingdao 266237, China*

ARTICLE INFO

Article history:
Received 5 May 2021
Revised 11 June 2021
Accepted 15 June 2021
Available online 21 June 2021

Keywords:
Photodynamic therapy
Nanophotosensitizer
Peptides
Self-assembly
Acid-activatable

ABSTRACT

A variety of nano-engineered photosensitizers have been developed for photodynamic therapy (PDT) of cancer diseases. However, traditional nano-engineering methods usually cannot avoid drug leakage and premature release, and have disadvantages such as low drug load and inaccurate release. The self-assembly strategy based on amphiphilic peptides has been considered to be more attractive nano-engineering method. Here we developed novel acid-activatable self-assembled nanophotosensitizers based on an amphiphilic peptide derivative. The peptide derivative was synthesized from a fluorescein molecule with thermally activated delayed fluorescence (TADF). The self-assembled nanophotosensitizers can specifically enter the tumor cells and disassemble inside lysosomes companied with "turn-on" fluorescence and photodynamic therapy effect. Such smart nanophotosensitizers will open new opportunities for cancer theranostics.

Photodynamic therapy (PDT) is an emerging method to treat tumors [1-4]. Compared with traditional cancer treatment methods, PDT has advantages such as non-invasion and less drug resistance [5]. Photosensitizers play a key role on the efficiency of PDT [6]. Till now, the clinical-used photosensitizers are mostly organic molecules which suffer from less accumulation in the targeted tumors.

With the continuous advancement of nanotechnology, a variety of nano-engineered photosensitizers [7] have been developed to specifically target and efficiently accumulate in tumor tissue based on different matrix like liposomes [8,9], polymers and silica [10]. However, these traditional nano-engineering methods have several disadvantages. First, it is difficult to avoid leakage or early release, which will lead to ineffective accumulation of photosensitizers in tumor tissue. Second, the synthetic ingredients used to prepare these nanophotosensitizers may be cytotoxic. Third, traditional nanoencapsulation methods usually do not have high drug loads [11]. Last, few of these nanophotosensitizers are designed to be activated smartly by tumor microenvironment.

To address these above-mentioned issues, the self-assembly strategy has been considered to be more attractive nano-engineering method [12-15], because self-assembling nanophotosensitizers usually have high atom economy and can be designed to have smart stimulus-responsive potentials [16-18]. Among various self-assembling monomers, amphiphilic peptides have received more and more attention [19-21]. Self-assembled nanostructures based on amphiphilic peptides have been widely used in biomedical fields such as tissue engineering and gene therapy due to their characteristics of good biocompatibility, low immunogenicity and easy availability [22].

Here we developed acid-activatable self-assembling nanophotosensitizers based on an amphiphilic peptide derivative. The peptide derivative was synthesized from a fluorescein molecule FL which was found to have TADF property by our group (Scheme 1) [23,24]. The fluorescein molecule FL was reported to be a good theranostic photosensitizer in our previous work with the characteristics of low cytotoxicity, good photostability, high fluorescence quantum yield and localization inside lysosome where is mild acid [25-27]. But like other organic photosensitizers, FL has the same disadvan-

---

* Corresponding authors.
E-mail addresses: Mir2yue2@163.com (W.-H. Zheng), songfl@dlut.edu.cn, songfl@sdu.edu.cn (F. Song).

https://doi.org/10.1016/j.cclet.2021.06.041
1001-8417/

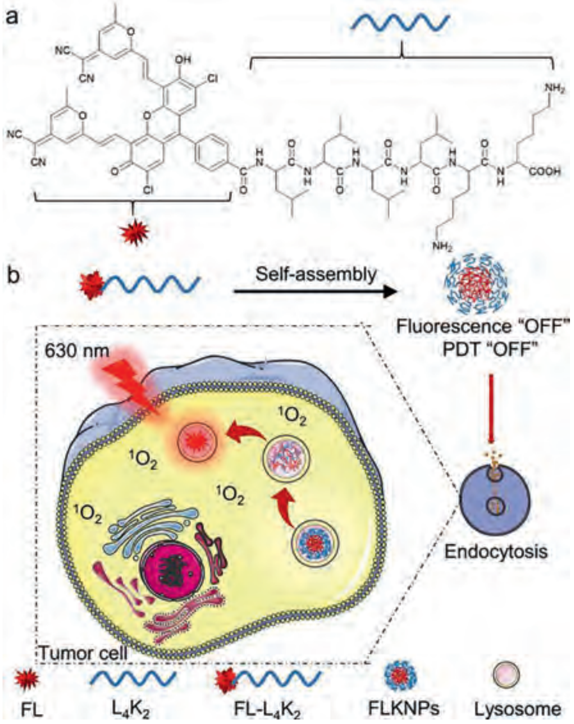

Scheme 1. (a) The molecular structure of FL-L_4K_2. (b) Schematic illustration of peptide nanophotosensitizers FLKNPs for efficient antitumor PDT.

tage of less accumulation in the targeted tumors. In this work, an amphiphilic hexapeptide L_4K_2 was linked to FL to form the FL-L_4K_2 which is the monomer of acid-activatable self-assembled nanophotosensitizers FLKNPs. Since FLKNPs contains only the hexapeptide L_4K_2 and the photosensitizer FL, the drug load can reach 50% according to the molecular weight contribution of the two parts. Importantly, the nanophotosensitizers FLKNPs are designed to selectively accumulate inside tumor cells and activated by mild acid condition in the lysosome. The fluorescence and PDT effect are expected to be "turned on" specifically in tumor cells for the purpose of theranostics.

The monomer FL-L_4K_2 was synthesized by the Fmoc peptide solid-phase synthesis method (Schemes S1 and S2 in Supporting information) and characterized by HRMS, ^{1}H NMR and HPLC (Figs. S1-S5 in Supporting information). And the absorption and fluorescence spectra of FL-L_4K_2 exhibited the almost same shape as those of FL (Fig. 1a; Fig. S6 in Supporting information), which further verified that FL-L_4K_2 was prepared correctly. Then FLKNPs was prepared by the self-assembly process of FL-L_4K_2. In detail, FL-L_4K_2 was dissolved in deionized water. The resulted solution was adjusted pH 8, followed by ultrasonicated for 15 min and left to stand for 24 h. Red precipitation can be observed to obtain the nanophotosensiters FLKNPs. The dynamic light scattering (DLS) data showed that the average hydrated diameter of the nanoparticles was about 153.5 nm (Fig. 1b), the zeta potential value +17.1 mV and the polydispersity index (PDI) 0.183. Transmission electron microscopy (TEM) images further confirmed that FLKNPs are spherical particles with an average particle size of about 130 nm (inset of Fig. 1b). In addition, the shape and size of the nanoparticles can keep good stability for at least 72 h according to the DLS data (Fig. S7 in Supporting information). Importantly, formation of FLKNPs led to the fluorescence quenching of FL-L_4K_2 (Fig. 1c), which gives chance to switch on fluorescence by stimulus-responsive strategy.

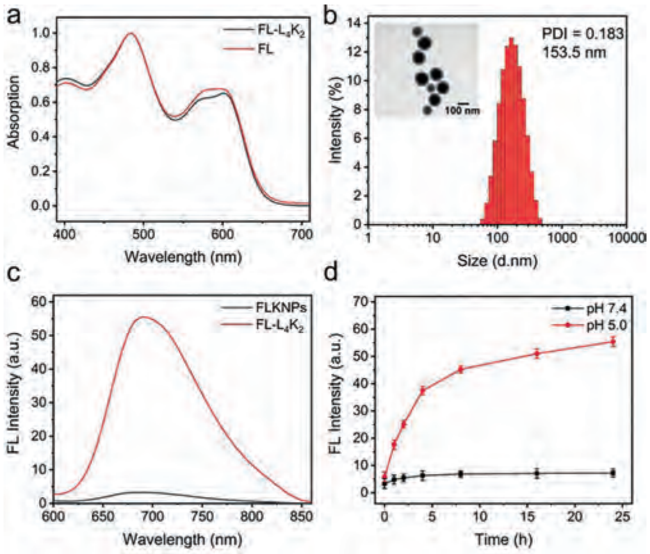

Fig. 1. (a) Normalized absorption spectra of FL and FL-L_4K_2 (5 μmol/L) in DMSO. (b) DLS measurement of FLKNPs and TEM image of FLKNPs. (c) Fluorescence spectra of 5 μmol/L FL-L_4K_2 and 10 μg/mL FLKNPs in PBS buffer. (d) The fluorescence intensity of FLKNPs changes with time under different pH conditions.

To verify the effect of turn-on fluorescence, we measured the fluorescence intensity of FLKNPs after incubated in aqueous PBS solutions with different pH (7.4, 7.0, 6.5, 6.0 5.5, 5.0, 4.5) for 24 h at room temperature. As shown in Fig. S8 (Supporting information), with the decrease of pH, the fluorescence intensity has a significant increase at pH 5.0 and pH 4.5. Then we measured the fluorescence intensity of FLKNPs under pH 7.4 and pH 5.0 in aqueous PBS solutions at different incubation time. As shown in Fig. 1d and Fig. S9 (Supporting information), the fluorescence intensity in pH 5.0 is significantly enhanced with time. But no obvious fluorescence change can be seen in pH 7.4. These results indicate that FLKNPs could dissemble at acidic environment. In fact, no particle size can be detected by DLS for the sample standing for 24 h at pH 5.0 (data not shown) which further verified that FLKNPs were completely decomposed at pH 5.0.

Besides the fluorescence turn-on effect, the PDT turn-on effect was also checked in solutions. TADF compound FL was known to be a triplet photosensitizer in our previous work. So, the nanosecond transient absorption spectra of FL-L_4K_2 and FLKNPs were recorded to check whether triplet excited state can also be achieved. As shown in Figs. 2a and b, the monomer possesses triplet excited state ($\tau = 8.90$). But no obvious triplet signal can be detected for FLKNPs (Fig. S10 in Supporting information). These results indicate that the PDT effect in FLKNPs should be encaged. The ROS production experiments further confirmed this speculation by using ABDA as a ROS indicator (Figs. 2c and d). The ROS can be generated in FL-L_4K_2 but not in FLKNPs. It means that the aggregation-induced quenching (ACQ) effect makes FLKNPs not only fluorescence quenched, but also PDT effect off. Meanwhile, the acid-treated FLKNPs can restore the ability of ROS generation (Fig. S11 in Supporting information). It suggests that the PDT effect could also be switched from off to on when FLKNPs dissemble in acid environment.

Further, the activation effect was checked in living cells. Fortunately, the fluorescence can be activated selectively by tumor cells (MCF-7 cells) but not by normal cells (COS-7 cells) (as shown in Fig. S12 in Supporting information). The selective activation can be attributed to the positive charge of the surface of FLKNPs. Compared with normal cells, tumor cell membranes have a higher proportion of negative charges [28], which can promote the selective

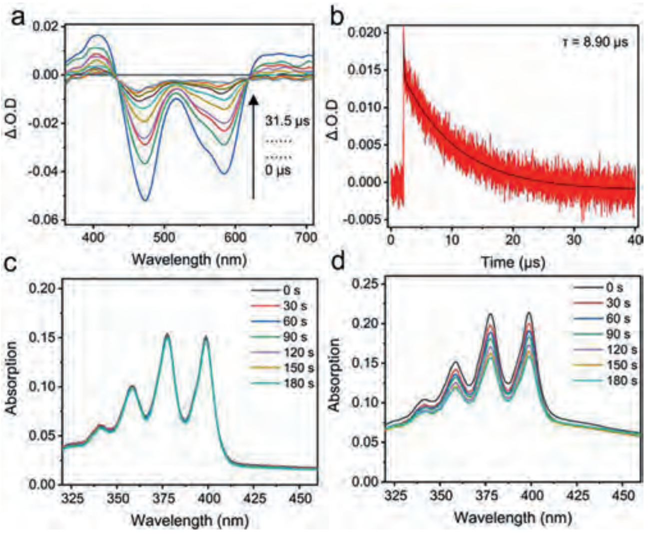

Fig. 2. (a) Nanosecond transient absorption spectra of FL-L_4K_2 (20 μmol/L) in deaerated ethanol at different decay times (λ_{ex} = 532 nm). (b) Decay trace of triplet state for FL-L_4K_2 (20 μmol/L) in deaerated ethanol (monitored at 646 nm, λ_{ex} = 532 nm). (c) Time-dependent absorption spectral changes seen for ABDA (10 μmol/L) and FLKNPs (7.36 μg/mL) with irradiation. (d) Time-dependent absorption spectral changes seen for ABDA (10 μmol/L) and FL-L_4K_2 (5 μmol/L) with irradiation.

endocytosis of FLKNPs by tumor cells through electrostatic interaction. The difference in the endocytosis rate of FLKNPs between normal cells and tumor cells may cause FLKNPs to accumulate in tumor cells and have lower toxicity to normal tissues. After endocytosis, it is reasonable to infer that FLKNPs can enter lysosomes and dissemble by the acid environment. Actually, the dissembling process was verified by the turn-on red fluorescence imaging in MCF-7 cells.

To explore the PDT activation effect of FLKPs in tumor cells, we used ROS indicator 2′,7′-dichlorodihydrofluorescein diacetate (DCFDA) to detect the ability of nanoparticles to generate ROS in cells. As shown in Figs. 3a-d, strong green fluorescence can only be observed in MCF-7 cells incubated with FLKNPs and light-treated. These results clearly prove that the PDT effect can be activated in tumor cells.

We used standard MTT analysis to determinate the phototoxicity and dark toxicity of FLKNPs (Figs. 3e and f). The dark toxicity of FLKNPs to MCF-7 cells is very low. Even at a high concentration of 120 μg/mL, the survival rate of tumor cells is still as high as 85%, which shows that FLKNPs have good biocompatibility. When irradiated with a 630 nm red LED light for 10 min, the cell survival rate had dropped to 30% at the concentration of 10 μg/mL. The low dark toxicity and strong phototoxicity indicate that FLKNPs have excellent PDT effects.

In order to further identify the activation mechanism, we used the commercial lysosome marker dye Lysotracker Green to perform a lysosomal colocalization experiment. In MCF-7 cells, the red fluorescence signal after nanoparticle endocytosis was superimposed with the green fluorescence of Lysotracker Green (Figs. 4a-c). The Pearson negative staining coefficient reached 0.92 (Fig. 4d). Therefore, the process of disintegration of nanoparticles should occur in the lysosomes by the acid environment thereof accompanied with fluorescence and PDT effect "turns on".

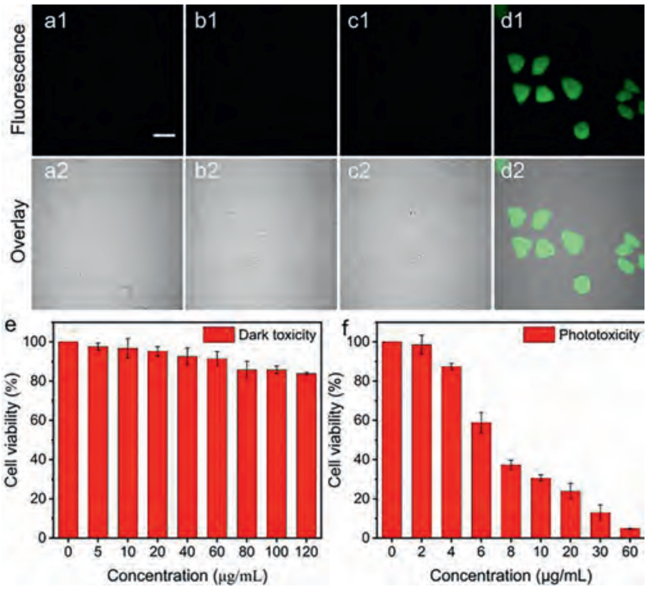

Fig. 3. Confocal images of intracellular ROS production (a) control group: no treatment, (b) with irradiation, (c) only incubated with 5 μg/mL FLKNPs, (d) incubated with 5 μg/mL FLKNPs and irradiation. (e) Cell viability of MCF-7 cells upon treatment with FLKNPs at different concentrations in the dark for 24 h. (f) Inhibition of the growth of MCF-7 cells in the presence of FLKNPs at different concentrations upon light irradiation (30 mW/cm^2, 10 min) followed by further incubation of the cells for 24 h. The data shown are mean values ± SD, $n = 3$. Scale bar: 30 μm.

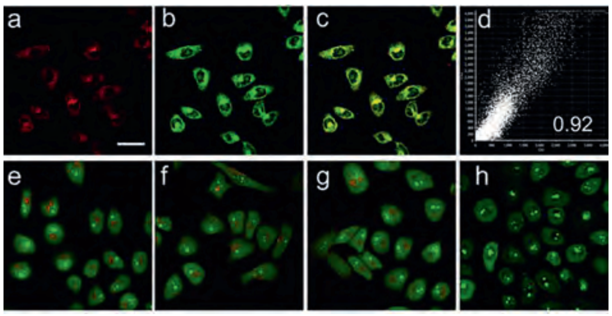

Fig. 4. Subcellular localization of FLKNPs in MCF-7 cells. (a) Fluorescence image of cells treated with FLKNPs (λ_{ex} = 488 nm; λ_{em} = 610–660 nm). (b) Fluorescence image of cells treated with Lysotracker Green (λ_{ex} = 488 nm; λ_{em} = 505–525 nm). (c) Overlay of images (a) and (b). (d) The Pearson negative staining coefficient. The acridine orange (AO) staining of MCF-7 cells without (e, g) or with (f, h) irradiation at the process of FLKNPs-mediated PDT, (g) only incubated with 10 μg/mL FLKNPs, (h) incubated with 10 μg/mL FLKNPs and irradiation. Scale bar: 30 μm.

During the PDT process, the activated nanophotosensitizers should destroy the lysosomes and induce cell apoptosis [29]. To verify the above PDT mechanism, we used acridine orang (AO) as an indicator to determine the integrity of the lysosome. As shown in Figs. 4e-h, the red fluorescence disappeared only in the group of the cells with FLKNPs and irradiation, which means that lysosomes were destroyed by PDT. The above results verify that FLKNPs can selectively enter tumor cells by endocytosis, dissemble in lysosomes, activate fluorescence and PDT, and induce cell apoptosis by destroying the lysosomes.

In summary, by rationally designing amphiphilic peptide monomer FL-L_4K_2 and inducing their self-assembly by adjusting pH, we can easily prepare activatable nanophotosensitizers FLKNPs as a theranostic system with a high drug loading rate of 50% for photodynamic therapy. FLKNPs are sensitive to acidic pH. The fluorescence of FLKNPs is "off" at pH 7.4. However, at pH 5.0, the nanoparticles disintegrate and the fluorescence “turns on”. Meanwhile, the ability of ROS generation was activated. FLKNPs were found to have excellent stability and negligible low toxicity. Owing to the character of positive charge on the surface of nanoparticles, FLKNPs can selectively enter MCF-7 tumor cells other than normal cells. The fluorescence and PDT effect can be activated by the acid environment inside lysosomes. We envision that this peptide nano-drug delivery system provides a new direction for new "smart" theranostic nano-drugs.

Declaration of competing interest

The authors declare that they have no known competing financial interests or personal relationships that could have appeared to influence the work reported in this paper.

Acknowledgments

This work was financially supported by the National Natural Science Foundation of China (No. 21877011), the Fundamental Research Funds for the Central Universities (No. DUT20YG119), and the Talent Fund of Shandong Collaborative Innovation Center of Eco-Chemical Engineering (No. XTCXYX03).

Supplementary materials

Supplementary material associated with this article can be found, in the online version, at doi:10.1016/j.cclet.2021.06.041.

References

[1] C.A. Robertson, D.H. Evans, H. Abrahamse, J. Photochem. Photobiol. B 96 (2009) 1–8.
[2] P. Agostinis, K. Berg, K.A. Cengel, et al., CA Cancer J. Clin. 61 (2011) 250–281.
[3] A.P. Castano, T.N. Demidova, M.R. Hamblin, Photodiagnosis Photodyn. Ther. 2 (2005) 1–23.
[4] J. Garcia-Zuazaga, K.D. Cooper, E.D. Baron, Expert Rev. Anticancer Ther. 5 (2005) 791–800.
[5] S.B. Brown, E.A. Brown, I. Walker, Lancet Oncol. 5 (2004) 497–508.
[6] M. Ethirajan, Y. Chen, P. Joshi, R.K. Pandey, Chem. Soc. Rev. 40 (2011) 340–362.
[7] D. Bechet, P. Couleaud, C. Frochot, et al., Trends Biotechnol. 26 (2008) 612–621.
[8] T. Shigehiro, J. Masuda, S. Saito, et al., Nanomaterials 7 (2017) 290.
[9] A.S. Derycke, P.A. de Witte, Adv. Drug Deliv. Rev. 56 (2004) 17–30.
[10] L. Jiao, Y. Liu, X. Zhang, et al., ACS Cent. Sci. 6 (2020) 747–759.
[11] M. Gary-Bobo, Y. Mir, C. Rouxel, et al., Angew. Chem. Int. Ed. 50 (2011) 11425–11429.
[12] X. Chen, Z. Hu, L. Zhou, et al., Nanoscale Horiz. 6 (2021) 33–42.
[13] C. Deng, Q. Zhang, J. Guo, X. Zhao, Z. Zhong, Adv. Drug Deliv. Rev. 160 (2020) 199–211.
[14] B. Dong, S. Du, C. Wang, et al., ACS Nano 13 (2019) 1421–1432.
[15] Y. Cong, L. Ji, Y.J. Gao, et al., Angew. Chem. Int. Ed. 58 (2019) 4632–4637.
[16] J. Gao, J. Zhan, Z. Yang, Adv. Mater. 32 (2020) e1805798.
[17] Y. Yuan, C.J. Zhang, M. Gao, et al., Angew. Chem. Int. Ed. 54 (2015) 1780–1786.
[18] B. Sun, R. Chang, S. Cao, et al., Angew. Chem. Int. Ed. 59 (2020) 20582–20588.
[19] A. Dehsorkhi, V. Castelletto, I.W. Hamley, J. Pept. Sci. 20 (2014) 453–467.
[20] X. Li, C. Cao, P. Wei, et al., ACS Appl. Mater. Inter. 11 (2019) 12327–12334.
[21] F. Qiu, Y. Chen, C. Tang, X. Zhao, Int. J. Nanomedicine 13 (2018) 5003–5022.
[22] M.J. Sis, M.J. Webber, Trends Pharmacol. Sci. 40 (2019) 747–762.
[23] X. Xiong, F. Song, J. Wang, et al., J. Am. Chem. Soc. 136 (2014) 9590–9597.
[24] X. Xiong, F. Song, S. Sun, J. Fan, X. Peng, Asian J. Org. Chem. 2 (2013) 145–149.
[25] W. Chen, F. Song, Chin. Chem. Lett. 30 (2019) 1717–1730.
[26] Z. Liu, W. Shi, G. Hong, et al., J. Control. Release 310 (2019) 1–10.
[27] Z. Liu, F. Song, W. Shi, et al., ACS Appl. Mater. Inter. 11 (2019) 15426–15435.
[28] L. Oliveira-Ferrer, K. Legler, K. Milde-Langosch, Semin. Cancer Biol. 44 (2017) 141–152.
[29] E. Buytaert, M. Dewaele, P. Agostinis, Biochim. Biophys. Acta 1776 (2007) 86–107.